



Controls on Water Levels and Salinity in a Barrier Island Mangrove, Indian River Lagoon, Florida

Christina E. Stringer · Mark C. Rains · Sarah Kruse ·
Dennis Whigham

Received: 12 August 2009 / Accepted: 26 March 2010 / Published online: 9 July 2010
© Society of Wetland Scientists 2010

Abstract We examined controls on water levels and salinity in a mangrove on a carbonate barrier island along the Indian River Lagoon, east-central Florida. Piezometers were installed at 19 sites throughout the area. Groundwater was sampled at 17 of these sites seasonally for three years. Head measurements were taken at the other two sites at 15-minute intervals for one year. Water levels in the mangrove are almost always lower than lagoon water levels. Spectral analysis of water levels showed that mangrove groundwater levels are not tidally influenced. Salinities vary spatially, with values of ~10 psu in uplands, ~30 psu in regularly-flushed mangroves, and ~75 psu in irregularly-flushed mangroves. Cation and anion concentrations and stable isotope compositions indicate that water salinities are largely controlled by enrichment due to evapotranspiration. A shore-perpendicular electrical resistivity survey showed that the freshwater lens is restricted to uplands and that hypersaline waters extend deeply below the mangrove. These results indicate that evapotranspiration lowers water levels in the mangrove, which causes Indian River Lagoon water to flow into the mangrove where it evapoconcentrates and descends, forming a thick layer of high-salinity water below the mangrove.

Keywords Conductivity · Electrical resistivity · Evapotranspiration · Hypersalinity · Salt pan

C. E. Stringer (✉) · M. C. Rains · S. Kruse
Department of Geology, University of South Florida,
Tampa, FL 33620, USA
e-mail: cestring@mail.usf.edu

D. Whigham
Smithsonian Environmental Research Center,
Edgewater, MD 21037, USA

Introduction

Mangroves, which cover ~240,000 km² of sheltered subtropical and tropical coasts between latitudes 24° north and south where mean annual temperatures are >20°C (Lugo 1990; Dawes 1998), provide numerous ecological functions as well as goods and services. Mangroves support estuarine and near-shore marine productivity, in part by providing critical habitat for juvenile fish and through the export of nutrient-rich water (McKee 1995; Rivera-Monroy et al. 1998) or plant, algal, or animal biomass (Zetina-Rejón et al. 2003). Mangroves also protect coastal habitats against the destructive forces of hurricanes, typhoons, and tsunamis (e.g., Kandasamy and Narayanasamy 2005; Granek and Ruttenberg 2007; Alongi 2008).

Hydrology is a master variable in coastal mangroves, directly or indirectly controlling ecosystem structure and function. Plant community composition can be controlled by salinity and/or water levels (Odum and McIvor 1990), while primary productivity is largely controlled by salinity, nutrients, and/or water levels (Feller 1995; Chen and Twilley 1999; Suarez and Medina 2005; Cardona-Olarte et al. 2006; Lovelock et al. 2007). Typically, primary productivity can be greatly enhanced by additions of nutrient-rich water (McKee 1995; Rivera-Monroy et al. 1998).

The hydrology of coastal wetlands is complex, with climatically and geologically controlled fluxes of fresh water interacting with oceanographically and geologically controlled fluxes of sea water. Water levels and fluxes can be controlled by tidal variations, which can be propagated rapidly through surface-water and ground-water environments (Hughes et al. 1998; Ataie-Ashtiani et al. 2001). However, water levels and fluxes also can be controlled by episodic direct precipitation and associated surface-water and ground-water inflows during storms (Hughes et al.

1998) and/or steady ground-water inflow between storms (Drexler and De Carlo 2002). In some cases, water levels and fluxes also can be controlled by evapotranspiration, which can draw down water levels in the mangroves and draw water in from the surrounding surface-water and ground-water environments (Hughes et al. 1998). In many coastal mangroves, natural hydrologic patterns have been modified for a variety of reasons. On the east coast of Florida, for example, most of the mangroves have been impounded for purposes of mosquito control or the creation of habitat for migratory and resident waterfowl (e.g., Montague et al. 1987).

Salinity and specific solute concentrations in coastal wetlands vary primarily as functions of water sources, and additionally as functions of evaporation and water-rock interaction. The salinity of direct precipitation is typically ~ 0.01 psu; the salinities of fresh surface water and ground water typically are ~ 0.03 – 0.60 psu; and the salinity of sea water is ~ 35 psu (Maidment 1993). Therefore, the degree of sea-water intrusion strongly controls salinity. However, solutes remain in solution when water evaporates, so salinity also may be greatly influenced by the rate at which water flows through the coastal wetlands and the rate at which water evaporates while in the coastal wetlands (Hughes et al. 1998; Twilley and Chen 1998).

This study is part of a broader series of investigations of the controls on species composition, primary productivity, and nutrient cycling in mangroves on a carbonate barrier island on the east-central coast of Florida. Our investigation is specifically focused on identifying and quantifying the controls on water levels and salinity, because there is little fresh water on the barrier island, infrequent tidal inundation over much of the mangrove, and greater than sea-water salinities in much of the mangrove. We hypothesized that evapotranspiration plays a major role in controlling water

levels and salinities, by lowering the water table in the mangrove and creating a hydraulic gradient that draws surface water and ground water from the lagoon into the mangrove.

Study Site

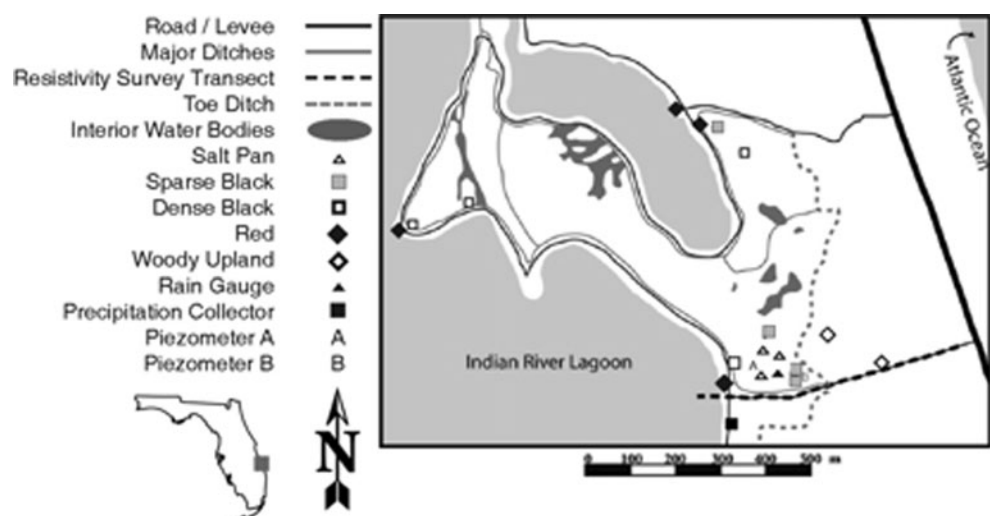
The study was conducted in SLC-24, a mosquito-control impoundment located at $N27^{\circ}33'$, $W80^{\circ}33'$ on the west shore of North Hutchinson Island. This barrier island is ~ 35 km in length and ~ 0.2 – 2 km in width, and is part of the system of barrier islands that bound the Indian River Lagoon, a 250-km estuarine system located on the east-central coast of Florida (Fig. 1). The study site is ~ 9 km north of the Ft. Pierce Inlet, the northern-most of five channels that connect the Atlantic Ocean and the Indian River Lagoon.

The impoundment was developed in 1970 when a dike was constructed around an existing mangrove-dominated wetland (Rey et al. 1990; Rey and Kain 1991). The impoundment was hydrologically isolated from the lagoon between 1970 and 1985. Tidal exchange was minimally restored in 1985 when a culvert was placed through the dike to remove water that had accumulated during two tropical storms. The culvert was later closed and the impoundment was again hydrologically isolated until 1987 when the culvert was reopened and four additional culverts were added.

The climate is subtropical (mean annual, maximum, and minimum temperatures are approximately 23, 28, and 18°C , respectively). Annual precipitation is approximately 1340 mm and it is distributed over a November–May dry season and a shorter June–October rainy season.

North Hutchinson Island sediments vary in size and texture, with a high concentration of shell debris and a mean CaCO_3 concentration of 65% (Wang and Horwitz 2007).

Fig. 1 Local setting showing piezometer and instrumentation locations, as well as resistivity transect position. Points described in legend as habitat types represent the piezometer nests located within that habitat



Vegetation cover in the impoundment decreased from 75% to near 30% between 1970 and 1985 but began to recover following the installation of the culverts in 1987 (Rey et al. 1990). Black mangrove (*Avicennia germinans* (L.) L.) is the dominant mangrove, but red (*Rhizophora mangle* L.) and white (*Laguncularia racemosa* (L.) C.F. Gaertn.) mangrove also are common. Buttonwood (*Conocarpus erectus* L.) also occurs, as do understory plants such as *Batis maritima* L., *Salicornia virginica* L., *Salicornia bigelovii* Torr., and *Borrchia frutescens* (L.) DC. The abundance, density, and sizes of mangroves vary across the impoundment from highly saline salt pans that have no mangroves or are fringed by dwarf black mangroves, areas that have dense and relatively short black mangroves, areas that have larger and more widely spaced black mangroves, to areas associated with open water where red mangroves are most abundant. Adjacent to and up gradient from the mangrove is a woody upland dominated by *Sabal palmetto* (Walter) Lodd. Ex Schult. & Schult. F. and *Schinus terebinthifolius* Raddi (Brazilian Peppertree). Therefore, for purposes of this study, five community types based on species composition and structure were identified: (1) salt pan, (2) sparse black mangrove, (3) dense black mangrove, (4) red mangrove, and (5) woody upland.

Methods

Physical Hydrology

Precipitation was measured continuously with a tipping-bucket rain gage (HOBO Event Rainfall Logger, Onset Computer, Pocasset, Massachusetts, USA). Stage in the Indian River Lagoon was modeled on 15-minute intervals using XTide 2 (<http://www.flaterco.com/xtide/index.html>), which was developed to predict tides and currents using an algorithm developed and used by the National Oceanic and Atmospheric Administration, National Ocean Service. The modeling program uses station-specific harmonic constants provided by the National Ocean Service and based on local tide gauge data, resulting in predictions that are accurate to ± 1 min and ± 0.03 m of measured high and low tides assuming no episodic storm-related surge (e.g., surge related to expansion of water during periods of extremely low pressure during the passage of extratropical storms).

Piezometers were installed at 19 locations. At 17 locations, 2.5 cm inside-diameter stainless-steel piezometers were installed in nests. These piezometers were screened over 15 cm beginning at 0.6, 1.2, and 1.8 m below the ground surface, with the exception of two sites in the woody upland that were screened over 15 cm beginning at 1.2 and 1.8 m below the ground surface. These piezometers were used for ground-water sampling. At two

locations, 5.0 cm inside-diameter PVC piezometers were installed. These piezometers were screened over 30 cm beginning at 2.0 m below the ground surface. Heads at these piezometers were measured on 15-minute intervals with pressure transducers and data loggers (Model 3001 Levelogger, Solinst, Georgetown, Ontario, Canada). The pressure transducers had a 1.5 m range and a ± 1 mm accuracy. Head data were compensated for changes in barometric pressure using barometric pressure data also measured on 15-minute intervals with a pressure transducer and data logger (Barologger, Solinst, Georgetown, Ontario, Canada).

Frequencies in the long-term water-level data from the piezometers and the Indian River Lagoon were determined using a fast Fourier Transform (FFT) algorithm in MATLAB (Version R2008A, Mathworks Inc., Natick, Massachusetts, USA). Prior to the FFT, a Tukey window function was applied to taper the data (Gubbins 2004). A Butterworth filter with a low-frequency cutoff of 33 hours was applied to the data to remove any long-term trends in the data. Mean daily head and stage cycles were also calculated using MATLAB.

Daily evapotranspiration was calculated by quantifying daily fluctuations in the long-term water-level record following the procedure outlined in White (1932). Daily evapotranspiration was computed as:

$$ET = S_y(24r \pm s)$$

where S_y is the specific yield of the sediments (10^{-1} in this setting), r is the rate of water table rise between 00:00 and 04:00, and s is the net change of the water level during the daily period (White 1932).

Chemical Hydrology

Water samples were collected and analyzed for temperature, pH, salinity, cations (e.g., Na^+ , K^+ , Mg^{2+} , Ca^{2+}), anions (Cl^- and SO_4^-), and stable isotopes (e.g., deuterium and oxygen-18) in the wet and dry seasons in 2005 and temperature, pH, and salinity in the wet and dry seasons in 2006 and 2007. Water samples were collected from the rain collector, the Indian River Lagoon, the primary perimeter ditch inside the impoundment, and piezometers in which water was found. The rain collector consisted of 1-L bottle contained within a plastic cylinder with a funnel top. A ping pong ball was placed in the funnel to limit evaporation. Rainfall sampling was opportunistic and immediately following rainfall, with only five samples collected throughout the study period.

Approximately three volumes of water were pumped from each piezometer prior to the collection of samples for chemical analyses. Samples were pumped through 0.45 μm in-line filters (Whatman, Maidstone, Kent, England) directly into pre-cleaned, acid-washed HDPE sample bottles. Anion samples were acidified with 1 ml

of nitric acid, and cation and anion samples were stored at the method-required range of 4 (± 2) °C prior to analyses. Stable isotope sample bottles were filled completely with negligible head space and sealed with Parafilm (American National Can, Chicago, Illinois, USA) to prevent the sample from equilibrating with ambient air.

Temperature, pH, and salinity of the surface-water and ground-water samples were measured in the field with a YSI 556 MPS (YSI Inc., Yellow Springs, Ohio, USA). Major cation and anion analyses were conducted at the University of South Florida Center for Water Analysis. Major cation concentrations were determined by inductively coupled plasma-emission spectroscopy following the EPA 200 method (Clesceri et al. 1998), and major anion concentrations were determined by ion chromatography following the EPA 300 method (Clesceri et al. 1998). Analytical precision of the laboratory analyses were better than 1%.

Stable isotope analyses were conducted at the UC Davis Department of Geology Stable Isotope Laboratory. Deuterium analyses were performed using the chromium reduction method (Donnelly et al. 2001), while oxygen-18 analyses were performed using the carbon dioxide equilibration technique (Epstein and Mayeda 1953). Deuterium and oxygen-18 are reported in the conventional, delta notation (δ):

$$\delta = \left(\frac{R_{\text{sample}}}{R_{\text{standard}}} - 1 \right) * 1000$$

where R is the ratio D/H or $^{18}\text{O}/^{16}\text{O}$ for deuterium and oxygen-18, respectively (Craig 1961). The resulting sample values of δD and $\delta^{18}\text{O}$ are reported in per mil (‰) deviation relative to Vienna Standard Mean Ocean Water (VSMOW) and, by convention the δD and $\delta^{18}\text{O}$ of VSMOW are set at 0‰ VSMOW (Gonfiantini 1978). Analytical precisions were $\pm 1.0\text{‰}$ and $\pm 0.05\text{‰}$ for δD and $\delta^{18}\text{O}$, respectively.

Evapoconcentration and Isotope Enrichment Modeling

Evapoconcentration is the process by which solute concentrations increase as water evaporates and solutes are retained in the remaining solution. An evapoconcentration model with Na^+ and Cl^- as conservative natural tracers was used to determine if evapoconcentration could explain solute concentrations within the five habitat types. The evapoconcentration model was run encompassing both dry and wet seasons, using seasonal mean Na^+ and Cl^- concentrations of the precipitation or Indian River Lagoon Water. The evapoconcentration model was:

$$C_{\text{RES}} = \frac{C_{\text{INI}}}{f_{\text{RES}}}$$

where C is the modeled Na^+ or Cl^- concentration in mg/L, f is the fraction of water remaining as it evaporates, and the subscripts ‘RES’ and ‘INI’ refer to residual water (e.g., evaporated ground-water in the mangrove) and initial water (e.g., precipitation or Indian River Lagoon Water), respectively.

Isotope enrichment due to evaporation is the process by which δD and $\delta^{18}\text{O}$ increase as water evaporates and heavier isotopes are retained in the remaining solution. Isotope enrichment was modeled through the application of a Rayleigh distillation model (Clark and Fritz 1997). The isotope enrichment model was:

$$R = R_0 f^{(\alpha-1)}$$

where R is the modeled isotope composition, R_0 is the initial isotope composition, f is the fraction of water remaining as it evaporates, and α is the equilibrium fractionation factor for evaporation (Majoube 1971). Kinetic effects due to high humidity were taken into account by applying a correction factor to the fractionation factor (Gonfiantini 1986). Two separate models were completed using theoretical precipitation and sea water as source waters. The precipitation source term was taken from the mean isotopic composition of precipitation at Kennedy Space Center, located ~113 km north and in the same physiographic region as the study site (http://www.uaa.alaska.edu/enri/usnip/isotope_1989-2001.cfm), while the sea water source term was taken from the isotopic composition for theoretical sea water (Gonfiantini 1978).

Resistivity Survey

A 400-m resistivity survey was conducted on an east-west transect from the Indian River Lagoon to the dune crest of North Hutchinson Island (Fig. 1). The shoreward half of the survey was completed on September 28, 2006 and the upland half on March 3, 2007. Data were collected using an Advanced Geosciences Incorporated Marine SuperSting R8 multichannel system connected to an external switching box that controlled the flow of current along the 56-electrode cable (AGI, Austin, Texas, USA). Electrodes (metal spikes) were spaced at 1.5 m intervals. Contact resistance was minimized as far as possible by driving the electrodes as deep as practical (typically ~20–30 cm deep) and watering the electrode-ground contact with sea water. Three individual surveys were completed, with a 20% overlap between surveys. Resistivity surveys measure terrain resistivity, which is a weighted average of the deposit and fluid resistivities. Therefore, resistivity is not solely a function of salinity. However, the extreme contrast in resistivity between fresh water (high resistivity/low conductivity) and sea water

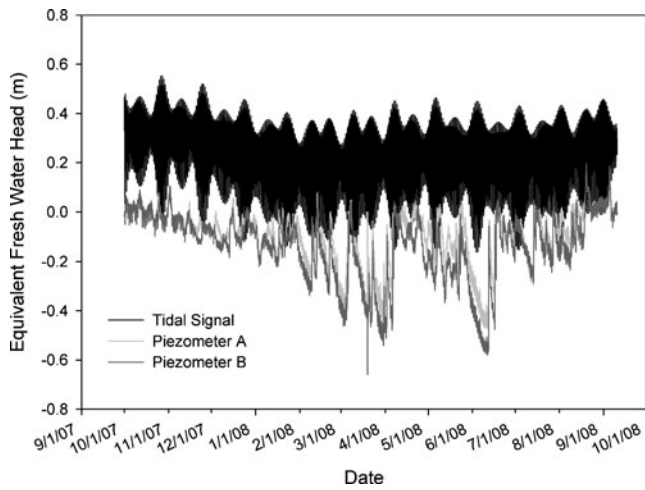


Fig. 2 Equivalent fresh-water head (m) of tide in the Indian River Lagoon and ground-water level in each of the piezometers

(low resistivity/high conductivity) makes the freshwater/sea water interface a strong component of measured terrain resistivities in any setting. Following acquisition, the data were inverted using the EarthImager 2D inversion software from Advanced Geosciences Incorporated.

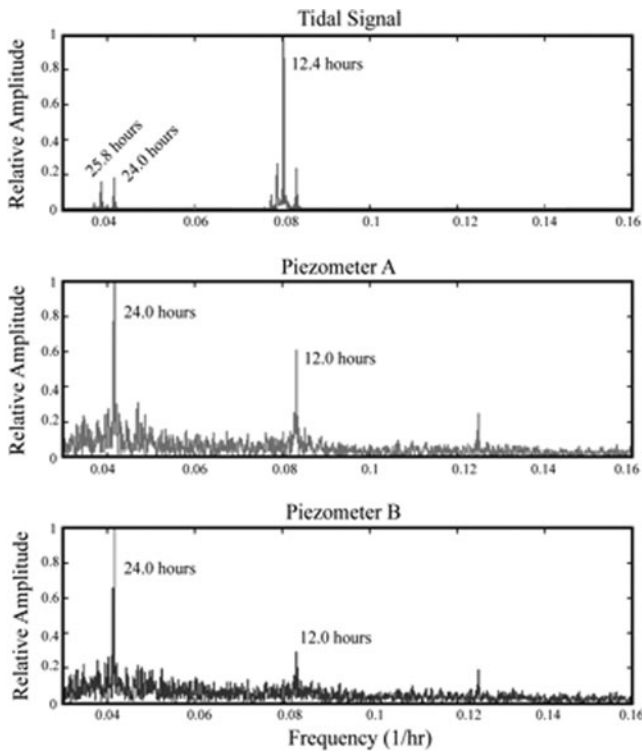


Fig. 3 Fourier transform results showing frequency spectra of equivalent fresh-water head data for the tide and piezometer ground-water levels. The y-axis shows the relative amplitude of the peaks, with the most intense peak having a value of 1. The x-axis is the frequency of the water-level pattern (1/hours)

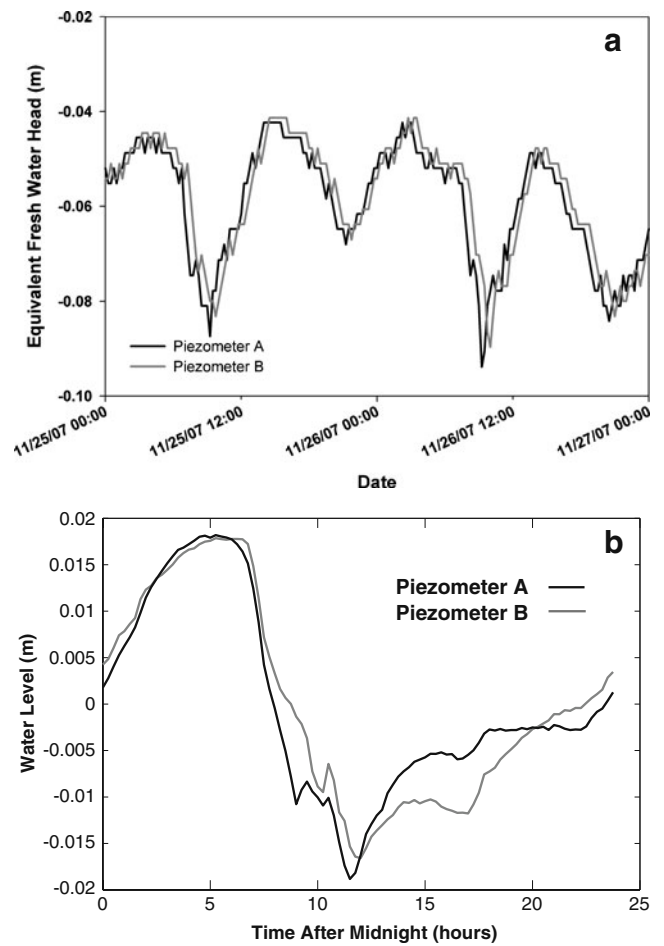


Fig. 4 a Representative long-term water level data from November 25–26, 2007 showing daily changes due to evapotranspiration. **b** Average daily cycle of entire equivalent fresh-water head (m) data set for the tide and piezometers showing lack of tidal influence on piezometer water levels. Y-axis is in the number of hours after midnight

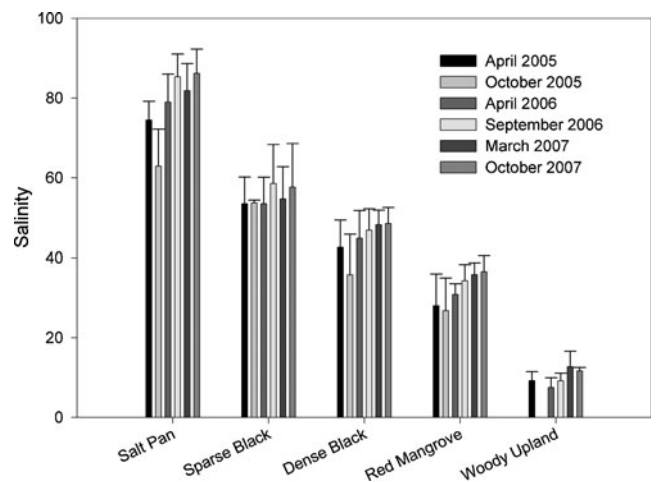


Fig. 5 Average ground-water salinity values for each wet and dry sampling event in each of the five habitat classifications. Bars are the average ground-water salinity for all depths at all sites sampled in that habitat and are arranged in ascending date from left to right. Error bars are the standard deviations of those averages ($\pm 1\sigma$)

Table 1 Average cation and anion concentration (ppm) and isotopic composition (‰) of each water type sampled during the investigation. Standard deviations shown are $\pm 1\sigma$. Isotopic aver-

ages for precipitation are long-term records at Kennedy Space Center, located ~113 km north and in the same physiographic region as the study site

Water Type	Na ⁺ (ppm)	K ⁺ (ppm)	Ca ²⁺ (ppm)	Mg ²⁺ (ppm)	Cl ⁻ (ppm)	SO ₄ ²⁻ (ppm)	δD (‰)	δ ¹⁸ O (‰)
Precipitation (<i>n</i> =5)	5±4	0.5±0.2	0.5±0.3	1±1	10±10	2±1	-20.8	-3.85
Surface Water (<i>n</i> =6)	8600±900	320±30	380±30	1100±100	15000±2000	2300±500	9±1	0.9±0.2
Salt Pan (<i>n</i> =18)	33480±60	1050±30	1020±10	4220±70	64000±1000	7800±400	8±2	1.4±0.5
Sparse Black (<i>n</i> =21)	23000±2000	750±90	1000±100	3000±200	42000±2000	5600±400	7±3	0.8±0.6
Dense Black (<i>n</i> =19)	16600±500	558±7	920±60	2260±60	31000±1000	4400±700	5±4	0.3±0.8
Red (<i>n</i> =12)	11200±500	410±10	600±100	1450±10	20500±500	2700±300	6±4	0.3±0.7
Woody Upland (<i>n</i> =9)	2500±700	112±2	210±60	350±30	4900±600	700±20	-15±5	-3.3±0.6

Results

Physical Hydrology

Raw water-level data were converted to equivalent freshwater head data to allow direct comparison of heads in fluids with varying densities. With the exception of a few excursions, heads in the mangrove habitats were lower than stages in the Indian River Lagoon (Fig. 2). Mean annual heads for the two continuously-monitored piezometers in the impoundment were -0.09 m and 0.02 m amsl, while mean annual stage of the Indian River Lagoon was 0.21 m amsl.

Spectral analysis of the piezometer and tidal data shows that the time frequencies of patterns in heads in the mangrove and Indian River Lagoon differ (Fig. 3). Heads in the mangrove have strong spectral peaks at 24.0 hours and weak spectral peaks at 12.0 hours, while stage in the Indian River Lagoon has a strong spectral peak at 12.4 hours and weak spectral peaks at 24.0 and 25.8 hours.

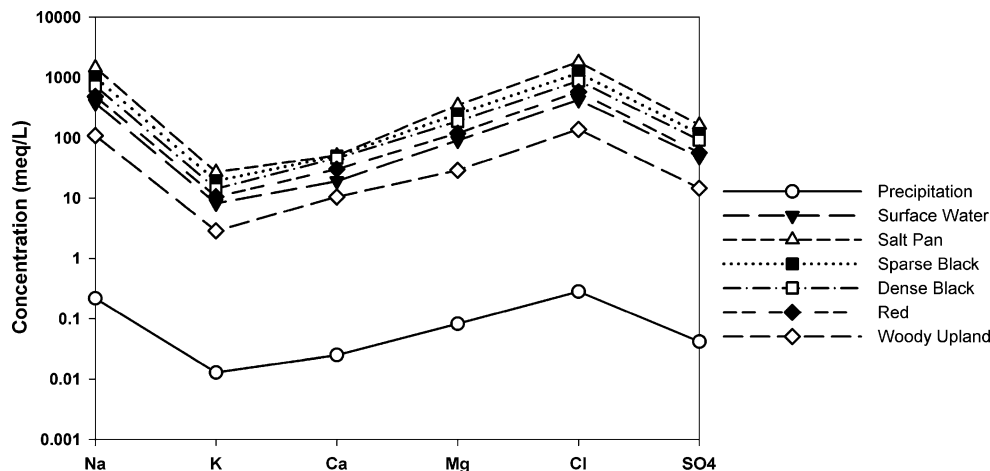
The direct effect of evapotranspiration on water levels can be seen in the examination of a segment of the long-term water-level record (Fig. 4a). The water-level data

between November 25, 2007 and November 26, 2007 show that heads decline from the early morning to a minimum at midday, and then recover through the afternoon and night to a maximum in the early morning. These water-level fluctuations correspond with daily evapotranspiration rates of 2 mm and 9 mm, which are within the range of evapotranspiration values (0–10 mm) reported for the Indian River Lagoon in the month of November from a previous study (Sumner and Belaine 2005). The same trend in water levels is found throughout the long-term record and can be seen in the mean daily head cycle (Fig. 4b).

Chemical Hydrology

Ground-water salinities varied by community type (Fig. 5). Mean±SD ground-water salinity was 78±9 psu in the salt pan (*n*=48), 55±2 psu in the sparse black mangrove (*n*=59), 44±5 psu in the dense black mangrove (*n*=56), 32±4 psu in the red mangrove (*n*=52), and 10±2 psu in the upland forest (*n*=19). Ground-water salinities varied significantly between community types (ANOVA, $p<0.01$; all Tukey post-hoc comparisons $p<0.01$) but showed no apparent seasonal or annual variations or trends throughout the course of the 2.5-year study.

Fig. 6 Schoeller diagram showing the average cation and anion concentrations (meq/L) of each water type collected in both the wet and dry seasons



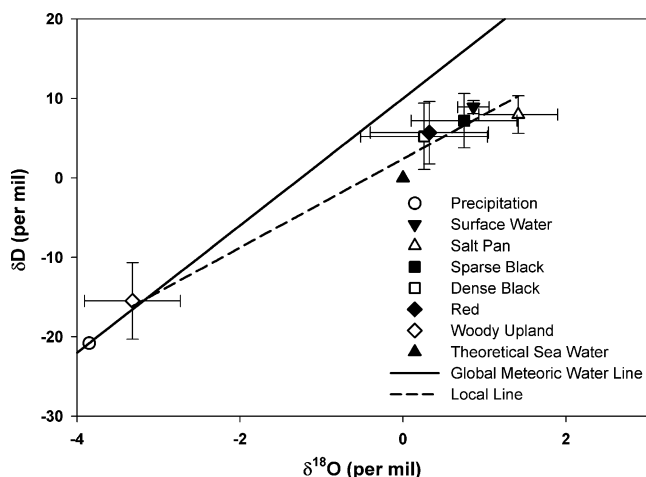


Fig. 7 δD and $\delta^{18}O$ (‰) of precipitation from long-term records at Kennedy Space Center, located ~113 km north and in the same physiographic region as the study site, theoretical sea water, and surface water and ground water collected during this study. The symbol shows the mean composition and the error bars represent the standard deviations ($\pm 1\sigma$) of those mean values. The solid black line is the global meteoric water line as defined by Craig (1961). The dashed line is the local evaporative trendline ($y=5.6x + 2.7$; $R^2=0.98$), determined via linear regression of the sample isotopic compositions

There were substantial differences in the absolute concentrations of the cations and anions in precipitation, surface water in the primary perimeter ditch inside the impoundment and the Indian River Lagoon, and ground water in each of the five community types (Table 1; Fig. 6). In all but one case (Ca^{2+}), cation and anion concentrations were greatest in salt pan ground water, followed by the sparse black mangrove ground water, dense black mangrove ground water, red mangrove ground water, surface water in the primary perimeter ditch inside the impoundment and Indian River Lagoon, woody upland ground water, and precipitation. Although the absolute concentrations varied, the relative proportions of the cations and anions were relatively constant across precipitation, surface water in the primary perimeter ditch inside the impoundment and Indian River Lagoon, and ground water in each of the five community types (Fig. 6).

Precipitation anion and cation concentration averages were comparable to those reported by the National Atmospheric Deposition Program monitoring location at Kennedy Space Center (<http://nadp.sws.uiuc.edu/sites/siteinfo.asp?id=FL99&net=NTN>). The cation and anion averages reported by the monitoring program all fall within the standard deviation of the averages of samples collected during this study.

Isotope data indicate that most of the surface water and ground water was evaporated (Fig. 7). Ground water in the woody upland had a mean isotopic composition of -15.49% and -3.32% for δD and $\delta^{18}O$, respectively, which plotted on the Global Meteoric Water Line (Craig 1961) near the mean

isotopic composition for regional precipitation (http://www.uaa.alaska.edu/enri/usnip/isotope_1989-2001.cfm). Surface water in the primary perimeter ditch inside the impoundment/Indian River Lagoon and ground water in the four

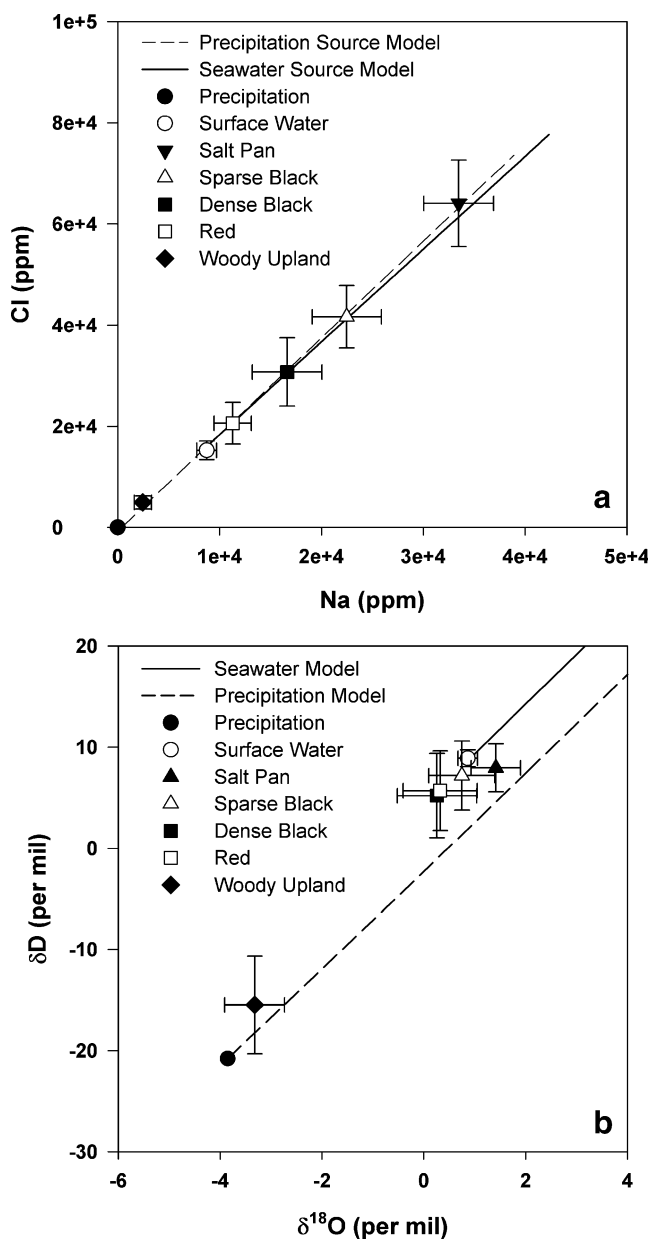
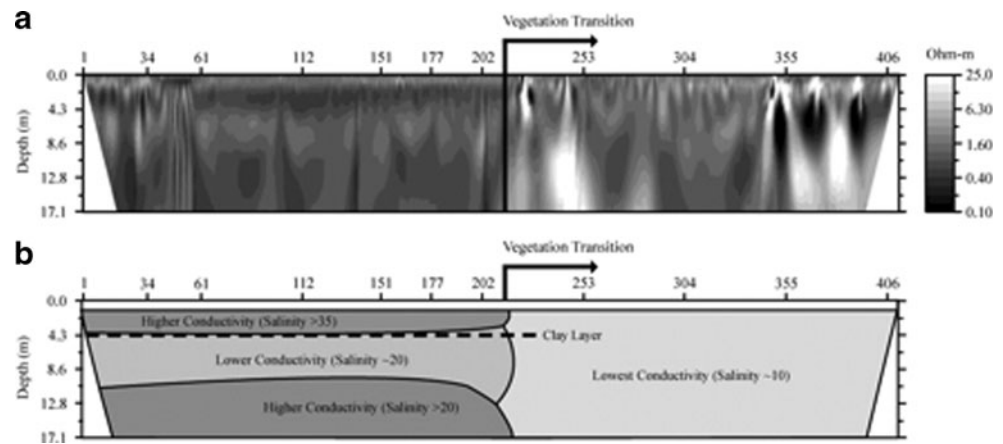


Fig. 8 **a** Evapoconcentration modeling results showing that sodium and chloride concentrations (ppm) in each of the community types can be achieved by evaporating precipitation and/or Indian River Lagoon water. The trendlines are the calculated increases in those concentrations, assuming that sodium:chloride ratio remains constant, as water is evaporated. **b** Isotope enrichment results showing that δD and $\delta^{18}O$ (‰) in each of the community types can be achieved through the Rayleigh distillation of precipitation and/or sea water. In both plots, the points represent the mean composition (sodium and chloride in Figure 8A and δD and $\delta^{18}O$ in Figure 8B) and the error bars represent the standard deviations ($\pm 1\sigma$) of those mean values

Fig. 9 **a** Profile showing resistivity inversion results. Horizontal axis is distance along the transect (m) from the coastline. Resistivities are shown in ohm-m. Black line and arrow indicate the transition from mangrove to upland vegetative communities. **b** General interpretation of resistivity results showing corresponding large-scale spatial patterns in conductivity. Dashed line represents a confining clay layer located under the mangrove that tapers out at the vegetative upland transition



remaining community types plotted along a local evaporative trend line that intersected the Global Meteoric Water Line near the mean isotopic composition for regional precipitation and the mean isotopic composition of sea water. The slope of this local evaporative trend line was 5.0, which is indicative of evaporation in an environment with a relative humidity of ~70%, which is the approximate mean annual humidity of this region (Southeast Regional Climate Center data for Vero Beach, Florida). Salt-pan ground water was the most evaporatively enriched, with mean isotopic composition of 7.95‰ and 1.41‰ for δD and $\delta^{18}O$, respectively.

Evapoconcentration and Isotope Enrichment Modeling

The evapoconcentration model results show that Na^+ and Cl^- concentrations in mangrove ground water can be produced through the evaporation of precipitation and/or Indian River Lagoon water (Fig. 8a). Mean Na^+ and Cl^- concentrations in the red mangrove, dense black mangrove, sparse black mangrove, and salt pan community types can be produced by evaporating >99% of the precipitation or 21%, 46%, 61%, and 74% of the Indian River Lagoon water, respectively. Similarly, the isotope enrichment model results also show that mangrove ground water can be produced through the evaporation of precipitation and/or Indian River Lagoon water (Fig. 8b). Mean isotopic compositions in the red mangrove, dense black mangrove, sparse black mangrove, and salt pan community types can be produced by evaporating 23%, 23%, 25%, and 28% of the precipitation, respectively, or 3%, 3%, 6% and 7% of the Indian River Lagoon water, respectively.

Resistivity

The resistivity results were somewhat noisy, most likely due to poor contact between electrodes and hard or resistive soils, but larger-scale spatial patterns were clear (Fig. 9). There was a discernable transition between the mangroves

(i.e., the salt pan, sparse black mangrove, dense black mangrove, and red mangrove) and the woody upland at a distance of approximately 220 m along the profile (Fig. 9). Below the mangrove, terrain resistivities were primarily ≤ 1 ohm-m to depths of at least 17 m, the maximum depth of the survey. Below the mangrove a lower-resistivity layer persists in the depth range of 1–4 m, thinning somewhat towards the woody uplands. Below the low resistivity layer lies a zone with higher resistivities between ~5–10 m depth. Any vertical stratification is less clear below the woody upland, where terrain resistivities are overall higher, with values generally ≥ 1 ohm-m.

Discussion

Annual water levels in the hydrologically altered impoundment appear to be largely controlled by evapotranspiration. Long-term water-level records show that water levels in the mangrove are generally lower than those in the Indian River

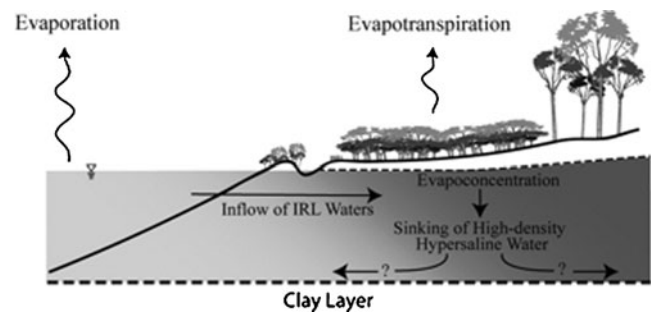


Fig. 10 Conceptual model showing importance of evapotranspiration in controlling water levels and salinities in the barrier island mangrove. As water evaporates a head gradient is created causing Indian River Lagoon water to flow into the mangrove. The high-density, hypersaline waters that result from the evapoconcentration sink and cause layering in the subsurface below the mangrove. The solid line represents the sub-marine and terrestrial land surface and the dashed line represents the clay layer that acts as a confining unit for the hypersaline waters

Lagoon (Fig. 2). Evaporation is likely higher in the Indian River Lagoon ($\sim 1500 \text{ mm year}^{-1}$) than evapotranspiration in the mangrove ($\sim 950 \text{ mm year}^{-1}$) (Twilley and Chen 1998; Sumner and Belaineh 2005). Nevertheless, drawdown is greater in the mangrove than in the Indian River Lagoon because (a) the Indian River Lagoon receives freshwater inflows from the mainland and sea-water inflows from the Atlantic Ocean and (b) the Indian River Lagoon has an effective specific yield of 10^0 while the mangrove sediments have a specific yield of 10^{-1} (Johnson 1967), which means that equal evapotranspiration will lead to a 10-fold greater drawdown in the mangrove. This greater drawdown in the mangrove maintains the hydraulic gradient from the Indian River Lagoon to the mangrove.

Daily water-level variations in the impoundment also appear to be largely controlled by evapotranspiration. The Indian River Lagoon Fourier spectrum shows a strong peak at 12.4 hours and weak peaks at 24.0 and 25.8 hours (Fig. 3). The 12.4-hour peak corresponds to the tide's diurnal cycle, while the 24.0 and 25.8 hour peaks correspond to the solar and lunar phases, respectively, of the tide's harmonic signal. The mangrove Fourier spectrum shows a strong peak at 24.0 hours and a weak peak at 12.0 hours (Fig. 3). The 12.4-hour peak corresponding to the tide's diurnal cycle and the 25.8 hour peak corresponding to the lunar phase of the tide's harmonic signal are not evident. The 24.0 hour peak corresponds to the daily solar cycle, which controls both the solar phase of the tide's harmonic signal and the mean daily peak evapotranspiration.

These peaks can be seen in the mean daily head and stage cycles (Fig. 4b). Mean stages in the Indian River Lagoon follow a sinusoidal curve, as might be expected for stages in a lagoon so close to a large inlet. Conversely, mean heads in the mangrove follow a pattern indicative of evapotranspiration control. Heads rise most steeply between 24:00 and 06:00 when plants are not transpiring, and decline most steeply between 06:00 and 12:00 when plants are transpiring. Interestingly, heads begin to rise after 12:00, although the rate at which they rise is slower than later in the evening. The transition between the heads declining and rising is abrupt. This suggests that evapotranspiration slows considerably and perhaps even ceases in some species in the afternoon, which results in the rate of inflow exceeding the rate of outflow (i.e., the rate of evapotranspiration). It has been shown that mangrove evapotranspiration rates decrease when salinities are increased (Ball and Farquhar 1984; Biber 2006). However, it is unclear if high salinity results in evapotranspiration rates that are generally lower throughout the day or in xylem dysfunction and evapotranspiration rates that are lower in the afternoon when atmospheric demand is highest (Tyree 1997). These results suggest the latter may be occurring,

although this is merely speculative and deserving of independent study.

The observed Na^+ and Cl^- concentrations and δD and $\delta^{18}\text{O}$ compositions can both be modeled by theoretically evaporating precipitation and/or Indian River Lagoon water (Fig. 8). However, the amount of evaporation necessary to model the observed Na^+ and Cl^- concentrations far exceeds the amount of evaporation necessary to model the observed δD and $\delta^{18}\text{O}$ compositions. This implies that transpiration plays an important role in controlling salinities because transpiration concentrates solutes by exclusion of solutes at the roots, extrusion of solutes from glands, and/or storage of solutes in leaves that ultimately drop and decompose (Dawes 1998), but does not result in isotope fractionation between the uptaken water and the remaining ground water (Gat 1996).

Collectively, these results indicate that evapotranspiration plays an important role in controlling water levels and salinities in the barrier island mangrove on the east-central coast of Florida (Fig. 10). Evapotranspiration lowers water levels in the mangrove, which creates a hydraulic gradient that drives water from the Indian River Lagoon to the mangrove. While infrequent tidal inundation of the mangrove does occur, the regular, daily pathway for this water movement is subsurface. Water evaporates and is transpired but solutes remain in solution, so mangrove water evapoconcentrates, becomes more dense, sinks, and creates the layering of high-salinity waters in the subsurface 1–4 m below the mangrove. However, the ultimate fate of the sinking, high-salinity water remains unclear.

Acknowledgments This study was supported by the Smithsonian Marine Sciences Network. This is contribution #811 from the Smithsonian Marine Station at Fort Pierce. Beth Fratesi, Kathryn Murphy, Pamela Stringer, Chris Reich, Jason Greenwood, and students in the USF Applied Geophysics course in Spring 2007 all helped with field data collection. We are grateful to Peter Swarzenski and the United States Geological Survey for the loan of the resistivity system and processing software. Jon Sumrall assisted by drafting Fig. 10.

References

- Alongi DM (2008) Mangrove forests: resilience, protection from tsunamis and responses to global climate change. *Estuarine Coastal and Shelf Science* 76:1–13
- Ataie-Ashtiani B, Volker RE, Lockington DA (2001) Tidal effects on groundwater dynamics in unconfined aquifers. *Hydrological Processes* 15:655–669
- Ball MC, Farquhar GD (1984) Photosynthetic and stomatal responses of two mangrove species, *Aegiceras corniculatum* and *Avicennia marina*, to long term salinity and humidity conditions. *Plant Physiology* 74:16
- Biber PD (2006) Measuring the effects of salinity stress in the red mangrove, *Rhizophora mangle* L. *African Journal of Agricultural Research* 1:1–4

- Cardona-Olarte P, Twilley RR, Krauss KW, Rivera-Monroy V (2006) Responses of neotropical mangrove seedlings grown in monoculture and mixed culture under treatments of hydroperiod and salinity. *Hydrobiologia* 569:325–341
- Chen R, Twilley RR (1999) Patterns of mangrove forest structure and soil nutrient dynamics along the Shark River Estuary, Florida. *Estuaries* 22:955–970
- Clark ID, Fritz P (1997) *Environmental isotopes in hydrogeology*. CRC Press LLC, Boca Raton
- Clesceri LS, Greenberg AE, Eaton AD (1998) *Standard methods for the examination of water and wastewater*, 20th edn. American Public Health Association, Washington
- Craig J (1961) Standard for reporting concentrations of deuterium and oxygen-18 in natural waters. *Science* 133:1833–1834
- Dawes CJ (1998) *Marine botany*, 1st edn. Wiley, New York
- Donnelly T, Waldron S, Tait A, Dougans J, Bearhop S (2001) Hydrogen isotope analysis of natural abundance and deuterium-enriched waters by reduction over chromium on-line to a dynamic dual inlet isotope-ratio mass spectrometer. *Rapid Communications in Mass Spectrometry* 15:1297–1303
- Drexler JZ, De Carlo EW (2002) Source water partitioning as a means of characterizing hydrological function in mangroves. *Wetlands Ecology and Management* 10:103–113
- Epstein S, Mayeda T (1953) Variation of O-18 content of waters from natural sources. *Geochemica et Cosmochimica Acta* 4:213–224
- Feller IC (1995) Effects of nutrient enrichment on growth and herbivory of dwarf red mangrove (*Rhizophora mangle*). *Ecological Monographs* 65:477–505
- Gat JR (1996) Oxygen and hydrogen isotopes in the hydrologic cycle. *Annual Review of Earth and Planetary Sciences* 24:225–262
- Gonfiantini R (1978) Standards for stable isotope measurements in natural compounds. *Nature* 271:534–536
- Gonfiantini R (1986) Environmental isotopes in lake studies. In: Fritz P, Fontes J CH (eds) *Handbook of Environmental Isotope Geochemistry 2*, Elsevier, New York, pp. 113–116
- Granek EF, Ruttenberg BI (2007) Protective capacity of mangroves during tropical storms: a case study from ‘Wilma’ and ‘Gamma’ in Belize. *Marine Ecology Progress Series* 343:101–105
- Gubbins D (2004) *Time series analysis and inverse theory for geophysicists*. Cambridge University Press, Cambridge
- Hughes CE, Binning P, Willgoose GR (1998) Characterisation of the hydrology of an estuarine wetland. *Journal of Hydrology* 211:34–49
- Johnson AI (1967) *Specific yield - compilation of specific yields for various materials*. U.S. Geological Survey Water-Supply Paper 1662-D. U.S. Government Printing Office, Washington, D.C
- Kandasamy K, Narayanasamy R (2005) Coastal mangrove forests mitigated tsunami. *Estuarine Coastal and Shelf Science* 65:601–606
- Lovelock CE, Feller IC, Ellis J, Schwarz AM, Hancock N, Nichols P, Sorrell B (2007) Mangrove growth in New Zealand estuaries: the role of nutrient enrichment at sites with contrasting rates of sedimentation. *Oecologia* 153:633–641
- Lugo AE (1990) Fringe wetlands. In: Lugo AE, Brinson MM, Brown S (eds) *Ecosystems of the world 15: forested wetlands*. Elsevier, Amsterdam, pp 143–169
- Maidment DR (ed) (1993) *Handbook of hydrology*. McGraw-Hill Inc., New York
- Majoube M (1971) Fractionnement en oxygène-18 et en deuterium entre l’eau et sa vapeur. *Journal of Chemical Physics* 197:1423–1436
- McKee KL (1995) Interspecific variation in growth, biomass partitioning, and defensive characteristics of neotropical mangrove seedlings: response to light and nutrient availability. *American Journal of Botany* 82:299–307
- Montague CL, Alexander VZ, Percival HF (1987) Ecological effects of coastal marsh impoundments: a review. *Environmental Management* 11:743–756
- Odum WE, McIvor CC (1990) Mangroves. In: Myers RL, Ewel JJ (eds) *Ecosystems of Florida*. University of Central Florida, Orlando, pp 517–548
- Rey J, Kain T (1991) *A guide to the salt marsh impoundments of Florida*. University of Florida, Florida Medical Entomology Laboratory
- Rey JR, Shaffer J, Crossman R, Tremain D (1990) Above-ground primary production in impounded, ditched, and natural Batis-Salicornia marshes along the Indian River Lagoon, Florida, USA. *Wetlands* 10:151–171
- Rivera-Monroy VH, Madden CJ, Day JW Jr, Twilley RR, Vera-Herrera F, Alvarez-Guillén H (1998) Seasonal coupling of a tropical mangrove forest and an estuarine water column: Enhancement of aquatic primary productivity. *Hydrobiologia* 379:41–53
- Suárez N, Medina E (2005) Salinity effect on plant growth and leaf demography of the mangrove, *Avicennia germinans* L. *Trees* 19:721–727
- Sumner DM, Belaine G (2005) Evaporation, precipitation, and associated salinity changes at a humid, subtropical estuary. *Estuaries* 28:844–855
- Twilley RR, Chen R (1998) A water budget and hydrology model of a basin mangrove forest in Rookery Bay, Florida. *Australian Journal of Freshwater and Marine Research* 49:309–323
- Tyree MT (1997) The Cohesion-Tension theory of sap ascent: current controversies. *Journal of Experimental Botany* 48:1753–1765
- Wang P, Horwitz MH (2007) Erosional and depositional characteristics of regional overwash deposits caused by multiple hurricanes. *Sedimentology* 54:545–564
- White WN (1932) *A method of estimating ground-water supplies based on discharge by plants and evaporation from soil: results of investigations in Escalante Valley, Utah*. US Geological Survey Water Supply Paper 659-A. US Government Printing Office, Washington, DC
- Zetina-Rejón MJ, Arreguín-Sánchez F, Chávez EA (2003) Trophic structure and flows of energy in the Huizache-Caimanero lagoon complex on the Pacific coast of Mexico. *Estuarine, Coastal and Shelf Science* 57:803–815